Hydrodeoxygenation of Propanoic Acid over Silica-Supported Palladium: Effect of Metal Particle Size

Yuliana K. Lugo-José, John R. Monnier, Andreas Heyden
and Christopher T. Williams*

Department of Chemical Engineering, University of South Carolina, Columbia, SC 29208

* To whom correspondence should be addressed:

Christopher T. Williams, Department of Chemical Engineering, Swearingen Engineering Center, University of South Carolina, Columbia, SC 29208, Phone: (803)777-0143, Fax: (803)777-8265, E-mail: willia84@cec.sc.edu

Supporting Information

S1.1 External/Internal Mass Transport Limitations

The absence of mass transport limitations under the conditions in the current study was confirmed. The diagnostic test for determining whether internal mass transport limitations were significant involved measurements using different mesh sizes of the catalyst. As shown in Figure S1, no change in the reaction rate for the different mesh sizes was observed for both Pd-2 and Pd-6, suggesting the absence of internal mass transfer limitations. These results are also consistent with previous calculations based on the Weisz-Prater criterion reported previously [1]. The absence of external mass transport limitations was confirmed by varying total flow rate (sccm) and measuring the reaction rate (Figure S2). The minimum flow rate where no external mass transport limitations were detected was 200 sccm. Therefore, all experiments were conducted at 200 sccm to ensure working under the kinetic regime.

In addition to the above tests, the effect of metal loading on activity was compared for the 4 (Pd-2) and 2.6 wt% Pd/SiO_2 (Pd-3), since they have similar particle size of 2 and 2.1 nm, respectively. As expected, the TOFs for Pd-2 and Pd-3 were in close agreement (0.46 and 0.51 min^{-1}, respectively). This indicates that the specific activity per Pd surface atom is independent on the weight loading (%) of the metal, confirming once again the absence of external and internal mass transfer limitations.

S1.2 X-ray Diffraction

The X-ray diffraction (XRD) patterns were recorded using a Rigaku Ultima IV diffractometer system with a D/tex Ultra detector with Cu Kα radiation (λ = 1.54 Å). Data were collected from 10-80º 2θ with a step size of 0.04º and a scan rate of 1º/min. Particle size was estimated using the Scherrer equation with LaB6 (NIST SRM 660a) as a reference for instrumental broadening. The XRD particle sizes were estimated for Pd-2, Pd-6 and Pd-10 for both the fresh and spent catalyst by using the Scherrer equation which is defined as:

$$d = \frac{K\lambda}{\beta\cos(\theta)}$$

Where d is the particle diameter, λ is the wavelength of the incident radiation, θ is the Bragg angle, β is the full width at half maximum (FWHM) of the diffracted peak, and *K* is the shape factor of the particle which is designated to be 1.0 for spherical particles, but could have values as low as 0.73 for triangular shaped particles.

Figure S3 shows the diffraction patterns for both fresh and spent Pd-2, Pd-6 and Pd-10. For each catalyst, three diffraction peaks were detected at 2θ = 40.1º, 46.7º, and 68.2º, which are indexed to the (111), (200), and (220) crystalline facets, respectively, of face-centered cubic (fcc) Pd according to the JCPDS card No. 05-0681 [2]**.** The broad peak at 2θ = 21º arises from the amorphous silica support. No significant peaks were detected for either the fresh or spent Pd-2 samples, indicating a particle size less than 2 nm and that there was no significant sintering. This is largely consistent with the chemisorption and STEM results. However, for Pd-6 and Pd-10, the particle sizes estimated by the Scherrer equation were 50-70% larger than the Sauter mean diameter estimated by STEM. The difference was even larger in the case of the chemisorption results for the Pd-6 samples. It should be noted that as the particle sizes increases, it is possible that the larger fraction of more sintered particles will result in narrower diffraction peaks, especially in a catalyst with very inhomogeneously distributed metal particles [3]. Indeed, discrepancy between chemsisorption, STEM and XRD have been observed by Punyawudho et al. [4] and Lambert et al. [5].

One of the reasons for these differences is also that XRD is a bulk technique that measures a volume-weighted mean diameter through the Scherrer equation [6]. In contrast, chemisorption is a surface-based approach and yields a surface-weighted mean diameter. In the case of STEM, to compare with chemisorption, the Sauter mean was used, $\overline{D}3,2 = \frac{\sum_i (Di^3)}{\sum_i (Di^2)}$ where Di is the diameter of the ith particle (Table S1). However, for comparison with XRD, the de Broukere mean diameter $\overline{D}4,3 = \frac{\sum_i (Di^4)}{\sum_i (Di^3)}$ is a more appropriate comparison. Table S1 shows that the STEM-derived de Broukere mean compares very well with the XRD particle size based on the Scherrer equation.

S1.3 X-ray Diffraction Patterns for Pd-2 to Pd-10

Additional powder XRD diffraction experiments were conducted for SiO_2 (S.A 330 m^2/g) and the Pd-2 through Pd-10 catalysts (Figure S4). The experiments were conducted to verify the crystallinity of the different Pd particle size. The X-ray diffraction patterns were recorded using a Rigaku MiniFlex II bench top system with a scintillation detector, and Kb filtered Cu Kα radiation (λ = 1.54 Å). The XRD patterns were compared to the ICDD reference spectra using the PDXL comprehensive analysis software. All spectra were taken at a scan rate of 0.5º/min. Particle size was estimated using the Scherrer equation as described above. For each catalyst, three diffraction peaks were detected at 2θ = 40.0º, 46.6º, and 68.2º, which are indexed to the (111), (200), and (220) crystalline facets, respectively. The broad peak at 2θ = 21º, corresponds to SiO_2 support. These patterns indicate the crystallinity of the Pd particles in the catalysts.

S1.4 High-Resolution STEM images for Pd-2 and Pd-6

STEM images were collected for Pd-2 and Pd-6 before the reaction. High resolution images with a focus of the crystallinity of the particles were obtained (see Figure S5). Based on the images it is seen that the small particles indeed have crystalline structure, which validates the assumption of Van Hardeveld and Hartog statistics for the surface crystalline planes.

Catalyst Id.	Pd loading (wt%)	Sauter		de Brouckere	
		d_{pd} (nm) O_2-H_2 titr.	d_{Pd} (nm) TEM	d_{Pd} (nm) XRD	d_{Pd} (nm) TEM
Pd-2b	2.0	2.0	2.7	<2.0	2.2
Pd-2a		-	2.8	<2.0	2.7
Pd-6b	1.9	3.8	5.1	12.1	11.2
Pd-6a		-	8.0	12.9	13.8
Pd-10b	3.3	12.4	12.1	14.7	16.2
Pd-10a		-	13.4	18.9	20.5

Table S1: Comparison of particle size Pd/SiO_2 over three different methods. [b] and [a] denotes before and after the reaction**.**

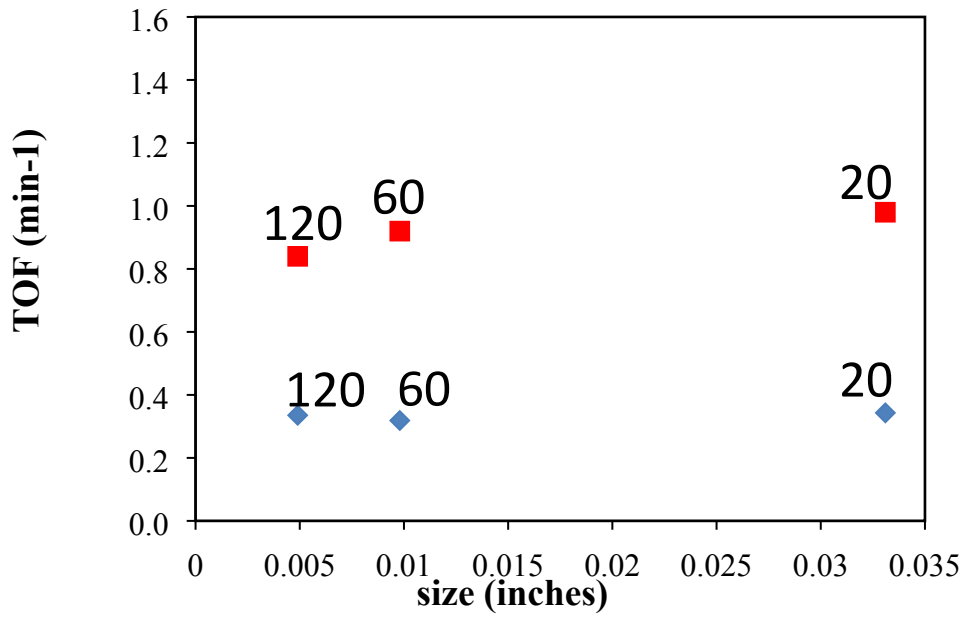

Figure S1. TOF vs. different mesh sizes of 4wt% Pd/SiO_2 (♦ Pd-2) and 1.9wt% Pd/SiO_2 (■ Pd-6) for HDO of PAc at 200 ºC and 1 atm. ~1.0 % PAc, 20% H_2/He, catalyst mass 200 mg , total flow 200 sccm, (20-120 mesh sizes).

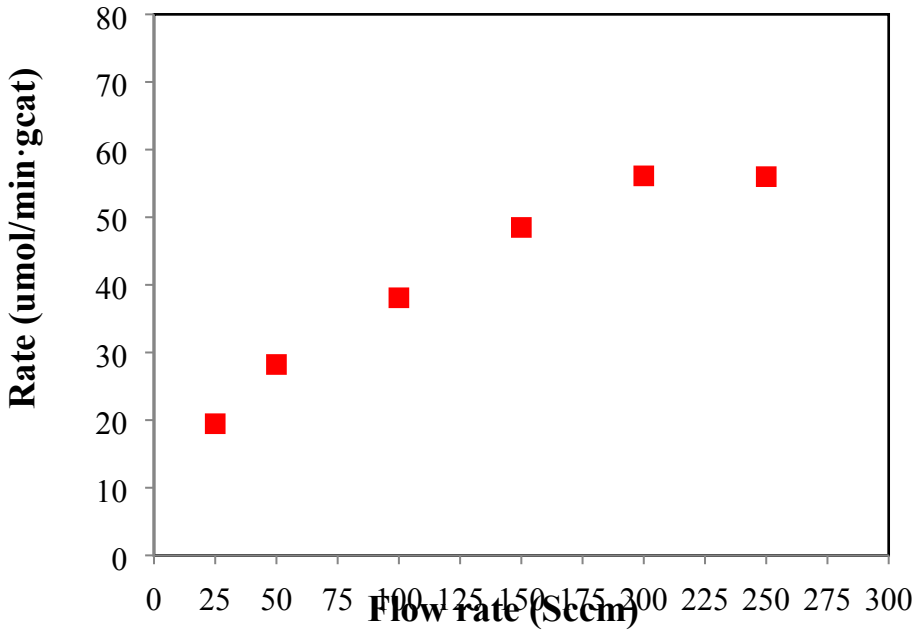

Figure S2. Reaction rate vs. flow rate (sscm) for 4wt% Pd/SiO_2 (Pd-2) for the HDO of PAc at 200 ºC and 1 atm. ~1.0 % PAc, 20% H_2/He, catalyst mass 200 mg , total flow 200 sccm.

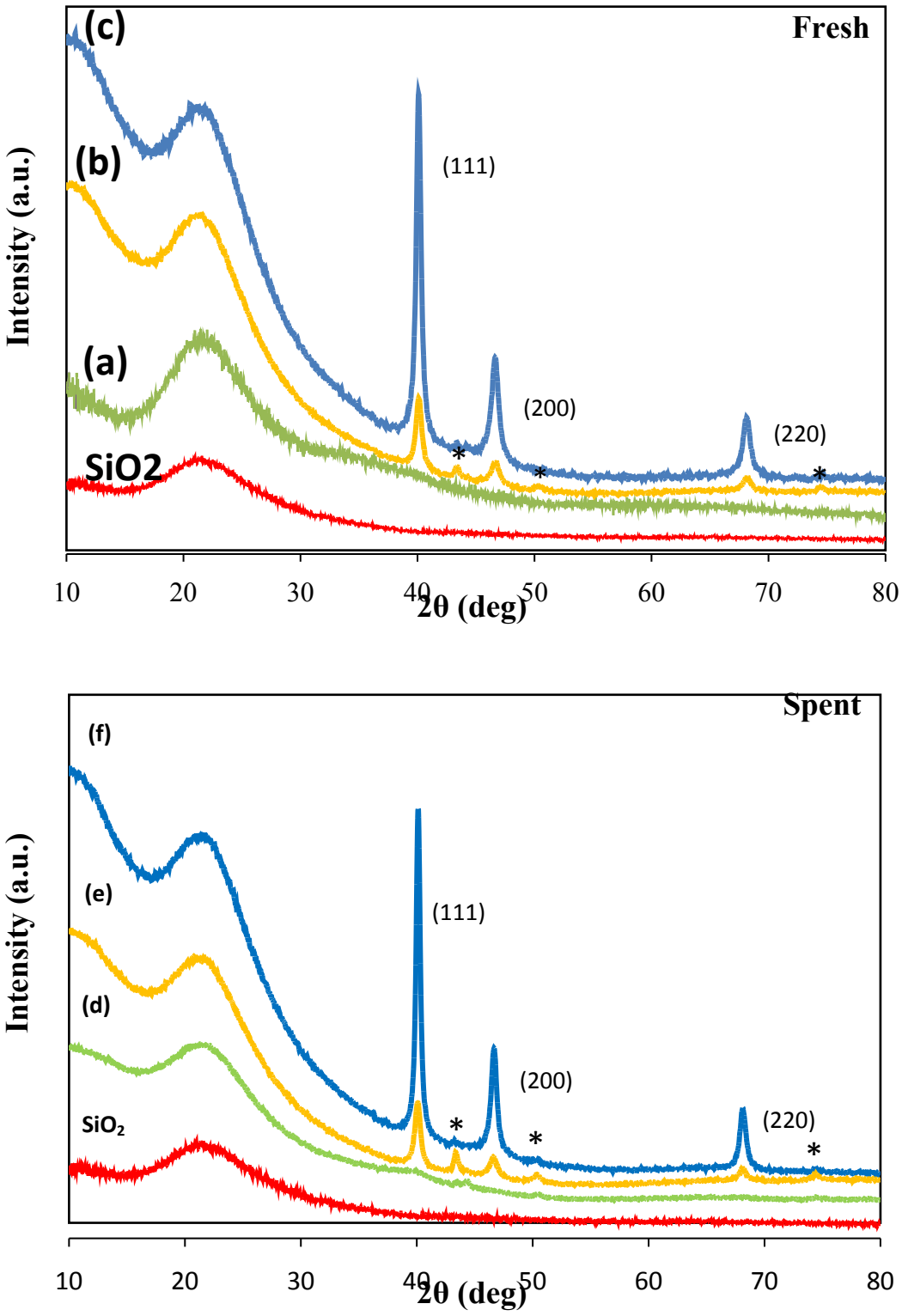

Figure S3: X-ray diffraction pattern for Pd/SiO_2, before: Pd-2 (a), Pd-6 (b), Pd-10 (c), and after the reaction: Pd-2 (d), Pd-6 (e) and Pd-10 (f). * Steel slide (background holder).

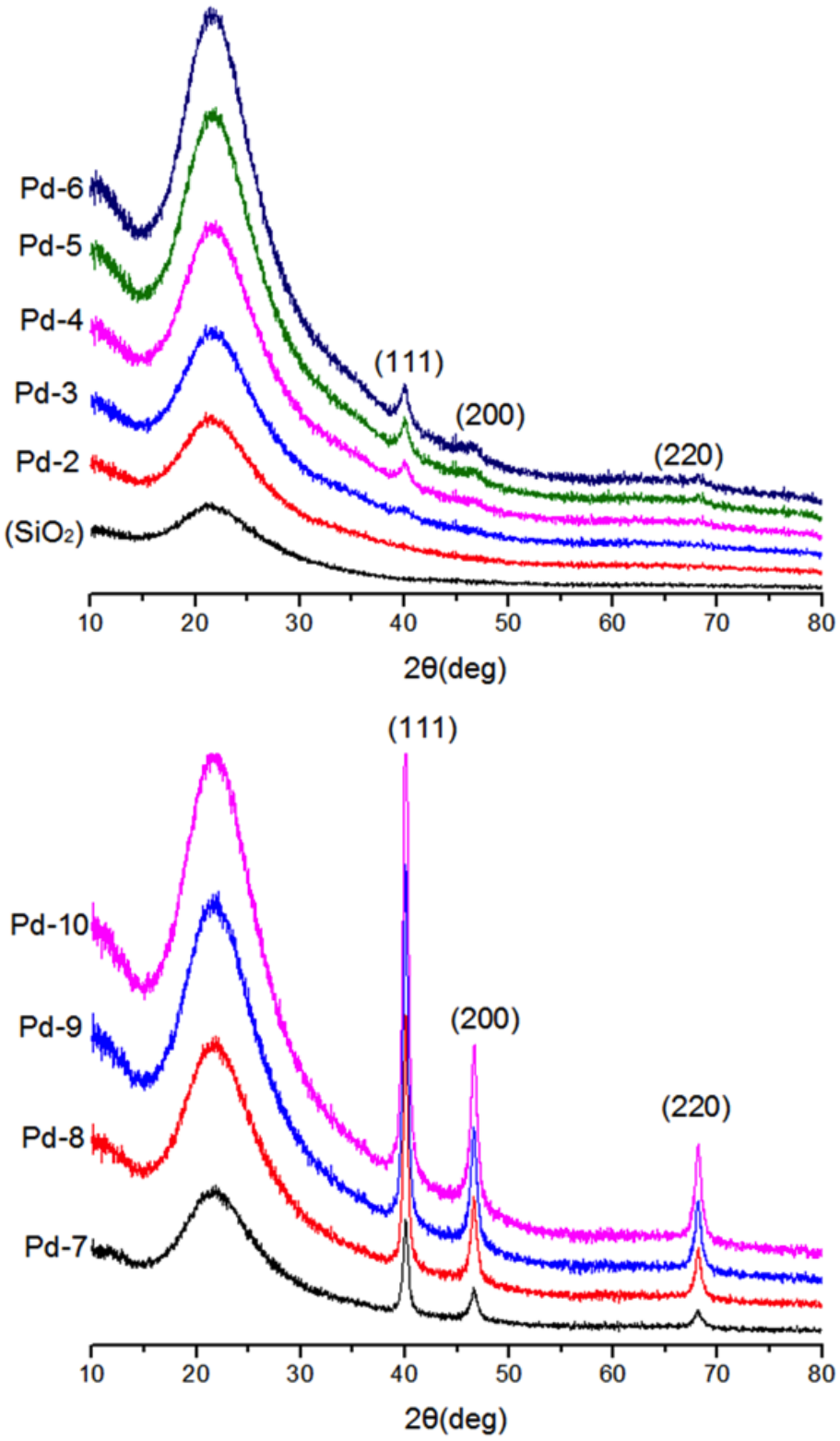

Figure S4: X-ray diffraction pattern for SiO_2 and Pd/SiO_2 (Pd-2 to Pd-10).

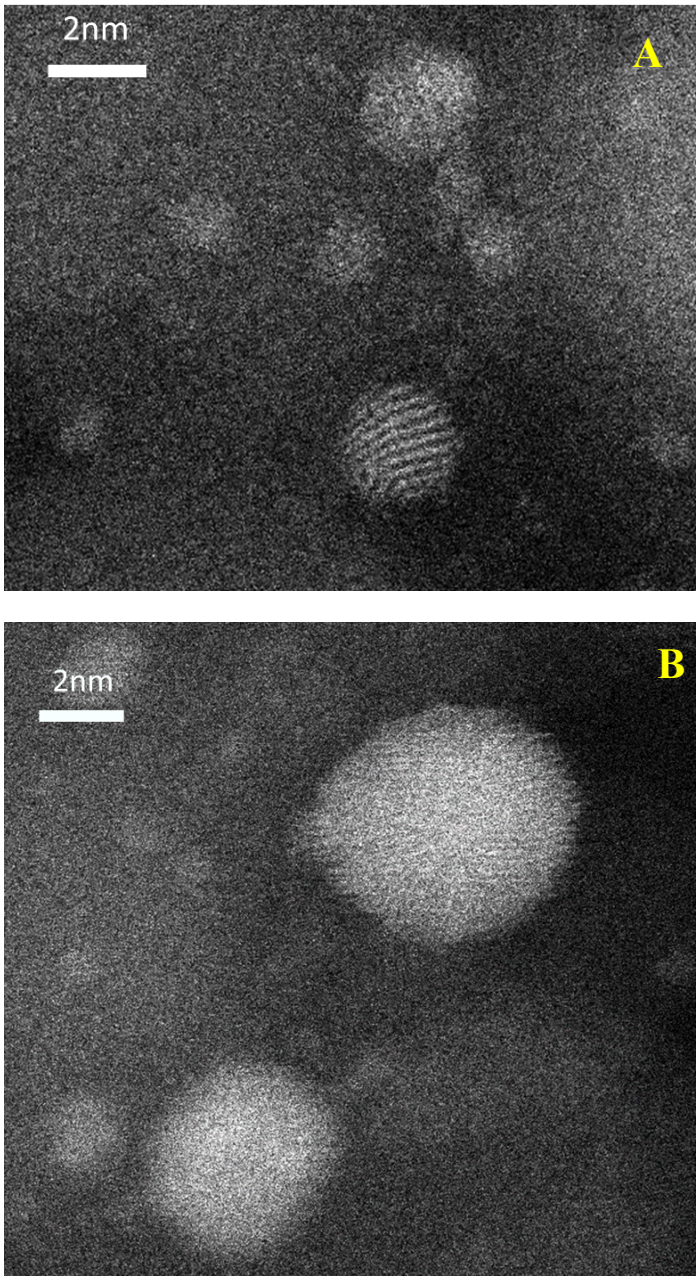

Figure S5: STEM images for Pd-2 (A) and Pd-6 (B) before the reaction.

Reference

[1] Y.K. Lugo-José, J.R. Monnier, C.T. Williams, Gas-phase, catalytic hydrodeoxygenation of propanoic acid, over supported group VIII noble metals: Metal and support effects, Applied Catalysis A: General, 469 (2014) 410-418.
[2] T. Shaochun, V. Sascha, Z. Zhou, R. Hua, M. Xiangkang, Facile and rapid synthesis of spherical porous palladium nanostructures with high catalytic activity for formic acid electro-oxidation, Nanotechnology, 23 (2012) 255606.
[3] X.-F. Yang, A. Wang, B. Qiao, J. Li, J. Liu, T. Zhang, Single-Atom Catalysts: A New Frontier in Heterogeneous Catalysis, Accounts of Chemical Research, 46 (2013) 1740-1748.
[4] K. Punyawudho, D.A. Blom, J.W. Van Zee, J.R. Monnier, Comparison of different methods for determination of Pt surface site concentrations for supported Pt electrocatalysts, Electrochimica Acta, 55 (2010) 5349-5356.
[5] S. Lambert, C. Cellier, P. Grange, J.-P. Pirard, B.t. Heinrichs, Synthesis of Pd/SiO_2, Ag/SiO_2, and Cu/SiO_2 cogelled xerogel catalysts: study of metal dispersion and catalytic activity, Journal of Catalysis, 221 (2004) 335-346.
[6] G. Bergeret, P. Gallezot, Particle Size and Dispersion Measurements, in: Handbook of Heterogeneous Catalysis, Wiley-VCH Verlag GmbH & Co. KGaA, 2008.